Supporting Information

Tafazzin deficiency impairs CoA-dependent oxidative metabolism in cardiac mitochondria

Catherine H. Le[1], Lindsay G. Benage[4], Kalyn S. Specht[2], Lance C. Li Puma[2], Christopher M. Mulligan[3], Adam L. Heuberger[5], Jessica Prenni[5], Steven M. Claypool[6], Kathryn C. Chatfield[7], Genevieve C. Sparagna[8], Adam J. Chicco[1-3*]

[1]Cell and Molecular Biology Program, Departments of [2]Biomedical Sciences, [3]Food Science and Human Nutrition, and [4]Biochemistry and Molecular Biology, [5]Horticulture and Landscape Architecture, Colorado State University, Fort Collins, CO, USA; [6]Department of Physiology, The Johns Hopkins University School of Medicine, Baltimore, MD; [7]Department of Pediatrics, University of Colorado School of Medicine, Children's Hospital Colorado Aurora, CO, USA; [8]Division of Cardiology, Department of Medicine, University of Colorado Anschutz Medical Campus, Aurora, CO, USA

Supplemental Methods

Mitochondrial Proteomic Profiling. Targeted analysis of mitochondrial metabolism proteins was performed in 30 μg of IF mitochondrial protein (N = 3/group) precipitated with acetone, resuspended in 8 M urea and 0.2% ProteaseMAX surfactant (Promega), reduced with dithiothreitol, and alkylated with idoacetamide. The proteins underwent tryptic digestion for 3 h at 37°C and then stopped with 0.5% trifluoroacetic acid. Peptides were dried in a speed-vac and purified using a reverse phase C18 TopTip (Glygen). Purified peptides were dried and reconstituted in 50 μl of 0.1% formic acid/3% acetonitrile.

Mass Spectrometry - Peptides were further purified and concentrated using an on-line enrichment column (Agilent Zorbax C18, 5 mm, 5 x 0.3 mm). Subsequent chromatographic separation was performed on a reverse phase nanospray column (Agilent 1100 nanoHPLC, Zorbax C18, 5 mm, 75 mm ID x 150 mm column) using a 90 minute linear gradient from 25%-55% buffer B (90% ACN, 0.1% formic acid) at a flow rate of 300 nanoliters/min. Peptides were eluted directly into the mass spectrometer (Thermo Scientific LTQ linear ion trap) and spectra were collected over a m/z range of 200-2000 Da using a dynamic exclusion limit of 3 MS/MS spectra of a given peptide mass for 30 s (exclusion duration of 90 s). Compound lists of the resulting spectra were generated using Xcalibur 2.2 software (Thermo Scientific) with an intensity threshold of 5,000 and 1 scan/group.

Data Analysis - MS/MS spectra were searched against the mouse Uniprot protein database (version 02/09/12) concatenated with reverse sequences for determination of the peptide FDR (118,690 sequence entries) using both the MASCOT database search engine (version 2.3) and Sorcerer™-SEQUEST® (1). Search parameters were as follows: average mass, parent ion mass tolerance of 2 Da, fragment ion mass tolerance of 1.5 Da, fully tryptic peptides with 1 missed cleavage, variable modification of oxidation of M and fixed modification of carbamidomethylation of C. Search results for each independently analyzed sample were imported and combined using probabilistic protein identification algorithms implemented in Scaffold software (Version 3.6.2, Proteome Software, Portland, OR) (2,3). Peptide and protein probability thresholds of 95% and 99% respectively, and a minimum of two unique peptides, were applied and resulted in a peptide FDR of 0.1% as calculated by Scaffold based on matches to reverse hits. Proteins containing shared peptides were grouped by Scaffold to satisfy the laws of parsimony. Manual validation of MS/MS spectra was performed for all protein identifications above the probability thresholds that were based on only two unique peptides. Criteria for manual validation included the following: 1) minimum of 80% coverage of theoretical y or b ions (at least 5 in consecutive order); 2) absence of prominent unassigned peaks greater than 5% of the maximum intensity; and 3) indicative residue specific fragmentation, such as intense ions N-terminal to proline and immediately C-terminal to aspartate and glutamate (used as additional parameters of confirmation.) Relative quantitation was determined by spectral counting (4). Raw spectral counts were normalized in Scaffold by applying a scaling factor such that the total spectral counts for each biological replicate are the same. A student's t-test was applied to calculate P-values. For relative

quantitation by spectral counting, the protein list was further filtered by the following criteria: proteins must be present in a minimum of 2 out of 3 biological replicates for a given state and the total normalized spectral counts for a given state must be > 10.

Cardiac amino acid and pantothenate analysis. Six male *Taz*^{KD} and WT mice were deeply anesthetized with sodium pentobarbital prior to rapid midline thoracotomy and freeze clamping of the beating heart with hemostats precooled in liquid nitrogen. Careful attention was placed on clamping the left ventricular free wall region within 5-10 seconds of entering the thorax. 30 mg of frozen heart wafer were homogenized in 1 mL of methanol/water (70:30) on ice and centrifuged at 3000xg for 10 min at 4 ºC, after which 800 µL of supernatant was transferred to a 1.5 mL microcentrifuge tube. The extract was dried using a speedvac, resuspended in 50 µL of pyridine containing 15 mg/mL of methoxyamine hydrochloride, incubated at 60ºC for 45 min, sonicated for 10 min, and incubated for an additional 45 min at 60ºC. Next, 50 µL of N-methyl-N-trimethylsilyltrifluoroacetamide with 1% trimethylchlorosilane (MSTFA + 1% TMCS, Thermo Scientific) was added and samples were incubated at 60 ºC for 30 min, centrifuged at 3000xg for 5 min, cooled to room temperature, and 80 µL of the supernatant was transferred to a 150 µL glass insert in a GC-MS autosampler vial. Metabolites were detected using a Trace GC Ultra coupled to a Thermo DSQ II (Thermo Scientific). Samples were injected in a 1:10 split ratio twice in discrete randomized blocks. Separation occurred using a 30 m TG-5MS column (Thermo Scientific, 0.25 mm i.d., 0.25 µm film thickness) with a 1.2 mL/min helium gas flow rate, and the program consisted of 80 ºC for 30 sec, a ramp of 15 ºC per min to 330 ºC, and an 8 min hold. Masses between 50-650 m/z were scanned at 5 scans/sec after electron impact ionization. For each sample, a matrix of molecular features as defined by retention time and mass (m/z) was generated using XCMS software standards (5). Features were normalized to total ion current, and the relative quantity of each molecular feature was determined by the mean area of the chromatographic peak among replicate injections (n=2). Molecular features were formed into peak groups using AMDIS software, and spectra were screened in the National Institute for Technology Standards (www.nist.gov) and Golm (http://gmd.mpimp-golm.mpg.de/) metabolite databases for identifications, validated by comparing retention times and mass spectra from heart extracts to commercial standards (6).

Measurement of cardiac tissue Acyl-CoAs. Acyl CoAs were extracted from mouse ventricular tissue samples by the method of Palladino et al (7), and quantified using liquid chromatography mass spectrometry on an API 4000 electrospray ionization mass spectrometer and an Acuity UPLC HILIC column (Waters, Milford, MA) with A solvent composed of 2% ammonium hydroxide in 50% methanol and B solvent composed of 5mM ammonium formate in methanol, pH 5. Runs were 12 minutes long with flow starting at 90% B, decreasing to 20% B at 2 minutes and back up to 90% B at 9 minutes. Samples were detected using neutral loss at m/z 507 and quantified using the ratio to three internal standards of different chain lengths for short, medium, and long chain acyl-CoAs respectively: 13C-Acetyl CoA, 13C-C8:0 CoA, and C17:0 CoA as detailed by Palladino et al (7).

Figure S1

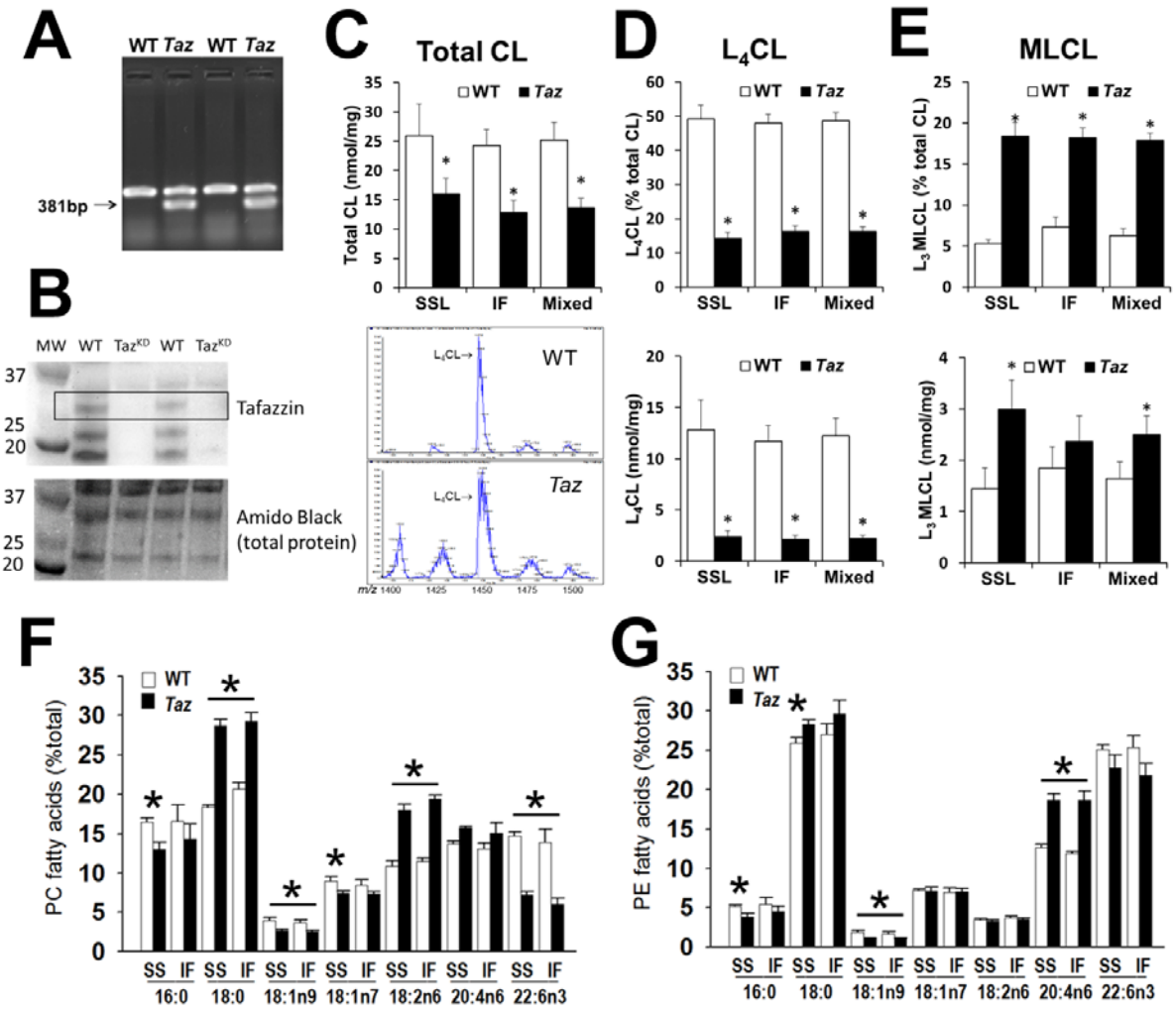

Figure S1. Cardiac mitochondrial phospholipid analysis of *Taz*^{KD} and WT mice.
(A) Representaive image of 381 bp *Taz* shRNA gene product present in offspring of *Taz*^{KD} mouse pairings genotyped by PCR analysis of tail DNA. **(B)** Representative immunoblot of WT and *Taz*^{KD} cardiac mitochondria for tafazzin protein (F-7 antibody # sc-365810; Santa Cruz Biotechnology) demonstrating absence of bands at the expected molecular weights of 25-34 kDa, and non-specific band at ~35 kDa. The boxed blots indicate those used for densitometric and statistical analyses presented in Figure 1 of the main manuscript. **(C)** Graphical summary (*N*=6/group) and representative MS spectra of total cardiolipin molecular species present in cardiac mitochondria isoalted from *Taz* and WT mice. Reltative proportion and total (per mg protein) mitochondrial contents of tetra-linoleoyl cardiolipin **(D)** and tri-linoleoyl monolysocardiolipin **(E)** in cardiac mitochondria from *Taz*^{KD} and WT mice determined by LC/MS (*N*=6/group). Fatty acid composition of phosphatiylcholine **(F)** and phosphatiylethanolamine **(G)** extracted from subsarcolemmal (SS) and intermyofibrillar (IF) cardiac mitochondria of *Taz*^{KD} and WT mice (*N*=4-6/group). **P* < 0.05 *Taz*^{KD} vs. WT by independent samples *t*-test.

Figure S2

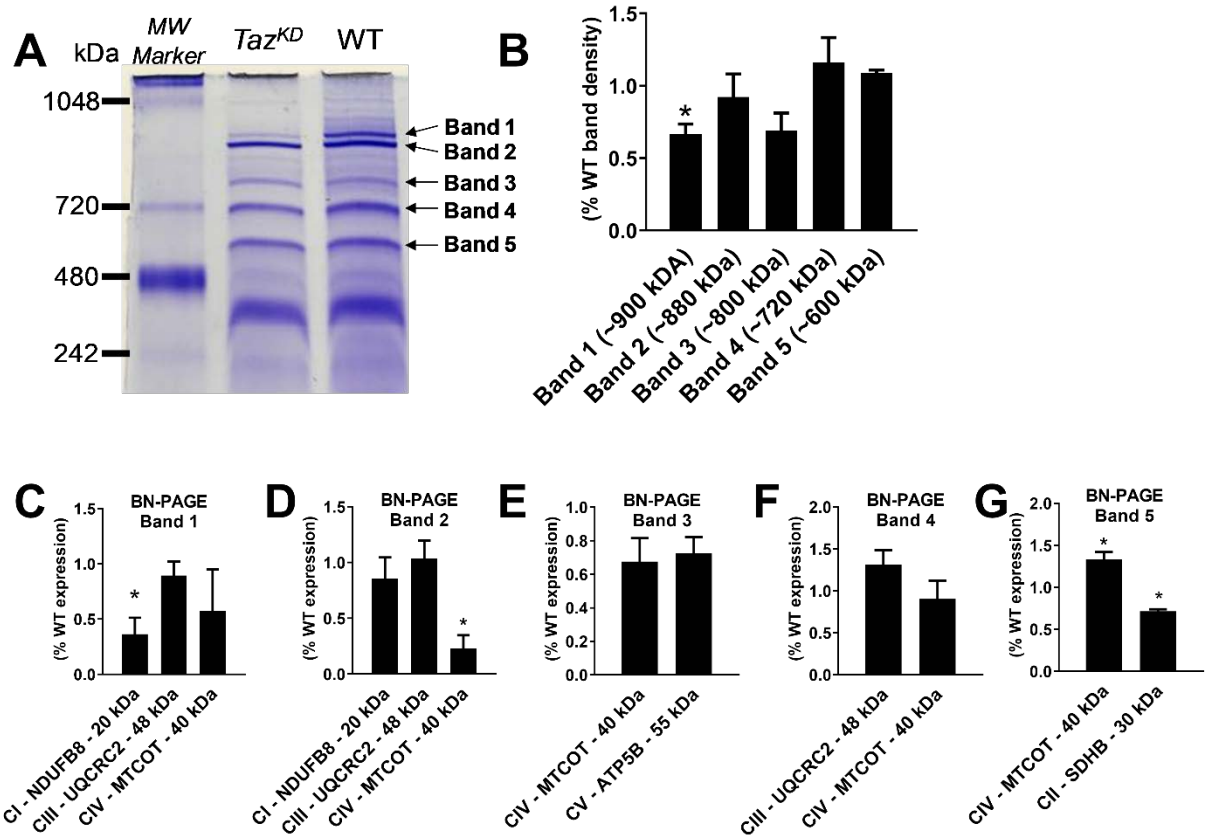

Figure S2. Analysis of high-molecular weight protein complexes in cardiac mitochondria from *Taz*^{KD} compared to WT mice. (A) Representative image of a Blue-Native PAGE stained gel separating high molecular weight (~500-1000 kDa) protein conglomerates from *Taz*^{KD} and WT mitochondria demonsrating lower band density in the highest MW (~900 kDa) band in *Taz*^{KD} vs. WT. **(B)** Densitometric analyses of BN-PAGE protein expression from *Taz*^{KD} relative to WT mitochondria from the same gels (N = 4/group) indicating trends for lower protein density in Bands 1 and 3 (* $P < 0.05$ vs. WT average). **(C-G)** Densitometric analysis of respiratory chain complex proteins separated from excised BN-PAGE gel bands 1-5 by subsequent SDS-PAGE and immunoblotting against antibodies for CI (NDUFB8), CII (SDHB), CIII (UQCRC2), CIV (MTCOT) and ATP Synthase (CV; ATP5B). *Taz*^{KD} band densities are expressed relative to WT band pairings from the same gel (*$P < 0.05$ vs. WT). Importantly, co-expression of subunits from different respiratory chain complexes does not necessarily indicate direct interaction. Results demonstrate loss a significant loss of CI and CIV from higher MW bands (**C and D**), suggesting their loss from higher MW respiratory chain "supercomplexes" reported previously in BTHS cell lines and this model. This is matched by significantly greater CIV protein found in lower MW bands (G), likely reflecting a greater dissociation of the complex into monomers. Complex II (SDHB) was also found to be lower in *Taz*^{KD} vs. WT ($P < 0.05$) in Band 5 **(G)**, consistent with the findings of Dudek et al. (8) and lower maximal CII-supported respiration in intact *Taz*^{KD} mitochondrial (Fig. 2C).

Table S1. Acyl-CoA levels in cardiac tissue from WT and *Taz*^{KD} mice by mass spectrometry expressed as % total acyl-CoA content.

CoA-ester species (% total)	WT			*Taz*^{KD}			*Taz*^{KD}/WT	*P value*
C2 Acetyl CoA	21.2	±	0.8	16.1	±	2.0	0.8	0.03
C3 Propionyl CoA	4.5	±	0.6	8.2	±	0.4	1.8	0.00
C4 3-OH C4 CoA & C3-DC Malonyl CoA	2.8	±	0.2	3.0	±	0.5	1.1	0.38
C4 Butyl CoA	7.3	±	1.1	10.3	±	0.6	1.4	0.03
C4-DC Acetoacetyl CoA& 3-Keto C4	3.5	±	0.5	7.3	±	1.3	2.1	0.02
C4-DC Succinyl CoA	0.7	±	0.2	1.0	±	0.2	1.5	0.16
C5-DC CoA & C6 3-OH CoA	1.2	±	0.2	1.1	±	0.1	1.0	0.44
C6 Hexanoyl CoA	6.4	±	0.7	8.7	±	1.4	1.4	0.10
C8 3-OH-C8 CoA	0.2	±	0.0	0.4	±	0.1	1.5	0.07
C8 Octanoyl CoA	0.6	±	0.1	0.8	±	0.1	1.4	0.03
C8:1 CoA	0.1	±	0.0	0.2	±	0.0	1.8	0.13
C10 3-OH-C10 CoA	0.4	±	0.1	0.5	±	0.1	1.3	0.13
C10 Decanoyl CoA	0.7	±	0.2	0.8	±	0.0	1.1	0.42
C10:1 CoA	0.5	±	0.0	4.6	±	0.6	9.3	0.00
C10:2 CoA	1.3	±	0.2	1.7	±	0.3	1.3	0.11
C10-DC Suberyl CoA	0.3	±	0.1	0.2	±	0.1	0.8	0.28
C12 3-Keto C12 CoA	0.3	±	0.0	0.2	±	0.0	0.7	0.02
C12 Dodecanoyl CoA	0.7	±	0.0	0.7	±	0.1	1.0	0.39
C12:1 CoA	0.0	±	0.0	0.1	±	0.1	3.9	0.05
C13 3-OH C12 CoA	0.3	±	0.0	0.2	±	0.0	0.8	0.08
C14 3-Keto C14 CoA	0.5	±	0.1	0.3	±	0.0	0.5	0.01
C14 3-OH-C14 CoA	0.8	±	0.1	0.4	±	0.1	0.5	0.01
C14:0 CoA	3.0	±	0.3	2.9	±	0.3	1.0	0.42
C14:1 CoA	4.3	±	0.3	3.5	±	0.7	0.8	0.17
C14:2 CoA	3.6	±	0.3	3.7	±	0.2	1.0	0.40
C16 3-OH-C16 CoA	3.1	±	0.4	6.1	±	0.6	1.9	0.00
C16 Palmitoyl CoA	2.7	±	0.2	2.0	±	0.3	0.8	0.07
C16:2 CoA	0.2	±	0.0	0.3	±	0.1	1.4	0.11
C16:1 Palmitoleoyl CoA	5.6	±	0.4	3.3	±	0.2	0.6	0.00
C16-DC-CoA	5.3	±	0.5	2.7	±	0.4	0.5	0.00
C18 3-Keto-C18-CoA	1.2	±	0.0	0.4	±	0.1	0.4	0.00
C18 Stearoyl CoA	1.5	±	0.1	0.9	±	0.1	0.6	0.00
C18:1 3-Keto C18:1 CoA	0.1	±	0.0	0.2	±	0.0	3.0	0.04
C18:1 Oleoyl CoA	1.1	±	0.3	0.3	±	0.0	0.2	0.01
C18:2 CoA	4.8	±	0.4	2.6	±	0.5	0.6	0.01
C18:3 CoA	6.8	±	0.7	2.5	±	0.4	0.4	0.00
C20 CoA	0.2	±	0.1	0.1	±	0.0	0.7	0.21
C20:1 CoA	0.2	±	0.0	0.2	±	0.0	1.0	0.47
C20:2 CoA	0.7	±	0.1	0.8	±	0.1	1.1	0.38
C20:3 CoA	0.6	±	0.1	0.1	±	0.0	0.2	0.00
C20:4 CoA	0.7	±	0.1	0.8	±	0.1	1.1	0.38

CoA molecular species are listed in order of carbon (C) chain length, then double bonds (C:X).Values are means ± SE expressed as % of total CoAs. *P* values are from independent sample *t*-test. DC, dicarboxyl;

Table S1 (cont.). Acyl-CoA profiling of cardiac tissue from WT and *Taz*^{KD} mice by mass spectrometry expressed as nmol/mg tissue.

CoA-ester species (nmol / mg tissue)	WT			*Taz*^{KD}			*Taz*^{KD}/WT	*P Value*
C2 Acetyl CoA	34.4	±	2.9	14.8	±	3.0	0.43	0.00
C3 Propionyl CoA	7.3	±	1.0	7.4	±	0.8	1.01	0.48
C4 3-OH C4 CoA & C3-DC Malonyl CoA	4.6	±	0.4	2.8	±	0.7	0.61	0.03
C4 Butyl CoA	11.6	±	1.5	9.3	±	1.3	0.80	0.14
C4-DC Acetoacetyl CoA& 3-Keto C4	5.7	±	0.9	6.8	±	1.8	1.19	0.30
C4-DC Succinyl CoA	1.0	±	0.3	0.9	±	0.2	0.88	0.38
C5-DC CoA & C6 3-OH CoA	1.9	±	0.4	1.0	±	0.1	0.53	0.03
C6 Hexanoyl CoA	10.3	±	1.0	7.6	±	1.0	0.74	0.05
C8 3-OH-C8 CoA	0.4	±	0.1	0.3	±	0.0	0.82	0.24
C8 Octanoyl CoA	0.9	±	0.1	0.7	±	0.0	0.76	0.05
C8:1 CoA	0.1	±	0.0	0.1	±	0.0	0.93	0.43
C10 3-OH-C10 CoA	0.6	±	0.1	0.4	±	0.0	0.71	0.13
C10 Decanoyl CoA	1.2	±	0.3	0.7	±	0.0	0.56	0.09
C10:1 CoA	0.8	±	0.1	4.2	±	0.8	5.19	0.00
C10:2 CoA	2.1	±	0.3	1.5	±	0.2	0.72	0.08
C10-DC Suberyl CoA	0.4	±	0.1	0.2	±	0.1	0.42	0.04
C12 3-Keto C12 CoA	0.4	±	0.0	0.2	±	0.0	0.41	0.00
C12 Dodecanoyl CoA	1.2	±	0.1	0.6	±	0.1	0.51	0.00
C12:1 CoA	0.1	±	0.0	0.1	±	0.0	2.24	0.12
C13 3-OH C12 CoA	0.5	±	0.1	0.2	±	0.0	0.43	0.00
C14 3-Keto C14 CoA	0.8	±	0.1	0.2	±	0.1	0.31	0.00
C14 3-OH-C14 CoA	1.3	±	0.2	0.4	±	0.1	0.30	0.01
C14:0 CoA	4.7	±	0.3	2.5	±	0.1	0.54	0.00
C14:1 CoA	7.0	±	0.8	3.0	±	0.4	0.43	0.00
C14:2 CoA	5.9	±	0.7	3.3	±	0.1	0.56	0.00
C16 3-OH-C16 CoA	5.0	±	0.4	5.3	±	0.2	1.06	0.25
C16 Palmitoyl CoA	4.3	±	0.5	1.8	±	0.2	0.41	0.00
C16:2 CoA	0.4	±	0.0	0.3	±	0.0	0.76	0.11
C16:1 Palmitoleoyl CoA	8.9	±	0.6	2.9	±	0.1	0.33	0.00
C16-DC-CoA	8.7	±	1.1	2.3	±	0.2	0.27	0.00
C18 3-Keto-C18-CoA	1.9	±	0.1	0.4	±	0.1	0.19	0.00
C18 Stearoyl CoA	2.5	±	0.0	0.8	±	0.1	0.33	0.00
C18:1 3-Keto C18:1 CoA	0.1	±	0.1	0.2	±	0.0	1.64	0.17
C18:1 Oleoyl CoA	1.7	±	0.5	0.2	±	0.0	0.13	0.01
C18:2 CoA	7.6	±	0.5	2.3	±	0.4	0.30	0.00
C18:3 CoA	11.2	±	1.6	2.1	±	0.2	0.19	0.00
C20 CoA	0.3	±	0.1	0.1	±	0.0	0.41	0.03
C20:1 CoA	0.3	±	0.1	0.2	±	0.0	0.54	0.03
C20:2 CoA	1.1	±	0.1	0.7	±	0.1	0.59	0.00
C20:3 CoA	1.0	±	0.2	0.1	±	0.0	0.08	0.00
C20:4 CoA	1.1	±	0.1	0.7	±	0.1	0.59	0.00

CoA molecular species are listed in order of carbon (C) chain length, then double bonds (C:X).Values are means ± SE in nmol/mg heart tissue. *P* values are from independent sample *t*-test. DC, dicarboxyl;

Table S2. Proteomic profiling of *Taz*^{KD} and WT mouse mitochondrial bioenergetics.

Identified Protein	#pep	Accession #	MW	*Taz*^{KD}/WT	*P* Value
NADH Dehydrogenase (Complex I)					
NDUFA3	**2**	**NDUA3_MOUSE**	**9 kDa**	**0.60**	**0.01**
NDUFA10	**6-14**	**NDUAA_MOUSE**	**41 kDa**	**0.68**	**0.01**
NDUFS5	**2-3**	**NDUS5_MOUSE**	**13 kDa**	**0.69**	**0.03**
NUDFA8	**4-7**	**NDUA8_MOUSE**	**20 kDa**	**0.60**	**0.03**
ND1	**2-3**	**NU1M_MOUSE**	**36 kDa**	**0.64**	**0.03**
NUDFA9	**9-17**	**NDUA9_MOUSE**	**43 kDa**	**0.72**	**0.04**
NDUFV1	8-14	D3YUM1_MOUSE (+1)	50 kDa	0.76	0.10
NDUFS3	7-10	NDUS3_MOUSE	30 kDa	0.82	0.10
NDUFA12	2-4	NDUAC_MOUSE	17 kDa	0.54	0.10
NDUFS2	10-16	NDUS2_MOUSE	53 kDa	0.70	0.11
NDUFA13	4-5	NDUAD_MOUSE	17 kDa	0.69	0.12
NDUFS1	13-21	NDUS1_MOUSE	80 kDa	0.86	0.15
ND5	2-3	NU5M_MOUSE (+1)	68 kDa	1.24	0.17
NDUFB10	4-8	NDUBA_MOUSE	21 kDa	0.89	0.18
NDUFB5	2-3	D3Z568_MOUSE (+1)	14 kDa	0.77	0.19
ND4	2-4	NU4M_MOUSE (+1)	52 kDa	0.87	0.19
NDUFB8	2-5	NDUB8_MOUSE	22 kDa	0.70	0.20
NDUFV3	2-3	NDUV3_MOUSE	12 kDa	0.81	0.20
NDUFC2	2-4	NDUC2_MOUSE	14 kDa	0.78	0.22
NDUFAB1	3-4	ACPM_MOUSE (+3)	17 kDa	0.86	0.22
NDUFB11	2-3	B1AV40_MOUSE (+1)	17 kDa	0.85	0.26
NDUFS4	3-4	E9QPX3_MOUSE (+1)	20 kDa	0.78	0.29
NDUFB6	3-4	A2AP31_MOUSE (+1)	16 kDa	1.14	0.31
NDUFV2	6-9	sp|Q9D6J6|NDUV2_MOUSE	27 kDa	1.07	0.31
NDUFS7	3-5	NDUS7_MOUSE	25 kDa	1.12	0.31
NDUFA6	2-3	NDUA6_MOUSE	15 kDa	0.89	0.35
NDUFA11	2-3	G5E814_MOUSE	15 kDa	1.09	0.41
NDUFS8	4-6	NDUS8_MOUSE (+1)	24 kDa	0.96	0.42
NDUFA5	2	D3YTQ8_MOUSE (+1)	9 kDa	1.02	0.47
NDUFB9	2-4	NDUB9_MOUSE	22 kDa	0.99	0.49
Total Complex I				**0.78**	**0.05**
Succinate dehydrogenase (Complex II)					
Subunit A	7-14	DHSA_MOUSE	73 kDa	0.82	0.07
Subunit B	4-5	A2AA77_MOUSE (+1)	32 kDa	1.09	0.32
Total Complex II				0.86	0.09
Cytochrome b-c1 (Complex III)					
Cytochrome b-c1 complex subunit 7	**2-4**	**Q9CQB4_MOUSE (+1)**	**14 kDa**	**0.80**	**0.03**
Isoform 2 of Cytochrome c1	**7-9**	**sp|Q9D0M3-2|CY1_MOUSE**	**29 kDa**	**1.31**	**0.04**
Cytochrome b-c1 complex subunit Rieske	5-8	UCRI_MOUSE	29 kDa	0.89	0.07
Cytochrome b-c1 complex subunit 1	15-17	QCR1_MOUSE	53 kDa	1.11	0.28
Cytochrome b-c1 complex subunit 8	2-3	QCR8_MOUSE	10 kDa	0.89	0.44
Cytochrome b-c1 complex subunit 2	16-17	QCR2_MOUSE	48 kDa	0.98	0.44
Total Complex III				1.06	0.31
Table S2 (cont.)	**#pep**	**Accession #**	**MW**	***Taz*^{KD}/WT**	***P* Value**

Cytochrome c oxidase (Complex IV)					
Cytochrome c oxidase subunit 5A	5-9	COX5A_MOUSE	16 kDa	0.79	0.12
Cytochrome c oxidase subunit 6C	2-4	COX6C_MOUSE	8 kDa	0.92	0.27
Cytochrome c oxidase subunit 5B	2-3	E9PWM0_MOUSE	14 kDa	0.84	0.34
Cytochrome c oxidase subunit 2	4-6	COX2_MOUSE (+1)	26 kDa	1.07	0.37
Cytochrome c, somatic	4-7	CYC_MOUSE (+2)	12 kDa	1.05	0.41
Cytochrome c oxidase subunit 6B1	4-6	CX6B1_MOUSE	10 kDa	0.99	0.48
Cytochrome c oxidase subunit IV isoform 1	4-9	A2RSV8_MOUSE (+1)	20 kDa	1.01	0.48
Total Complex IV				0.93	0.26
ATP Synthase (Complex V)					
ATP synthase subunit delta	2-4	ATPD_MOUSE (+1)	18 kDa	0.78	0.25
ATP synthase subunit g	2-4	ATP5L_MOUSE	11 kDa	0.83	0.17
ATP synthase subunit e2	2	ATP5I_MOUSE	8 kDa	1.27	0.18
ATP synthase subunit alpha	17-21	ATPA_MOUSE	60 kDa	0.90	0.19
ATP synthase subunit beta	23-30	ATPB_MOUSE	56 kDa	0.98	0.22
ATP synthase subunit d	8-10	ATP5H_MOUSE (+1)	19 kDa	0.91	0.28
ATP synthase gamma chain1	5-8	A2AKU9_MOUSE (+3)	33 kDa	0.87	0.29
ATP synthase subunit b	8-9	AT5F1_MOUSE (+1)	29 kDa	0.86	0.29
ATP synthase-coupling factor 6	2-4	ATP5J_MOUSE	12 kDa	1.08	0.32
ATP synthase subunit f	2	ATPK_MOUSE (+1)	10 kDa	0.97	0.41
ATP synthase protein 8	2	ATP8_MOUSE (+1)	8 kDa	1.30	0.10
ATP synthase subunit O	7-8	ATPO_MOUSE	23 kDa	1.02	0.43
Total ATP Synthase				1.00	0.46
Fatty acid oxidation (FAO)					
Medium-chain specific acyl-CoA dehydrogenase	**11-13**	**ACADM_MOUSE**	**46 kDa**	**0.68**	**0.03**
2,4-dienoyl-CoA reductase	**6-10**	**DECR_MOUSE (+1)**	**36 kDa**	**0.74**	**0.03**
Trifunctional enzyme subunit beta	**17-20**	**ECHB_MOUSE**	**51 kDa**	**1.20**	**0.03**
Long-chain-fatty-acid--CoA ligase 1	**2-6**	**ACSL1_MOUSE (+1)**	**78 kDa**	**0.44**	**0.04**
Very long-chain specific acyl-CoA dehydrogenase	**11-16**	**ACADV_MOUSE (+1)**	**71 kDa**	**0.89**	**0.05**
Delta(3,5)-Delta(2,4)-dienoyl-CoA isomerase	**2-6**	**ECH1_MOUSE**	**36 kDa**	**0.85**	**0.05**
3-ketoacyl-CoA thiolase	15-18	THIM_MOUSE	42 kDa	0.75	0.06
Hydroxyacyl-coenzyme A dehydrogenase	7-10	HCDH_MOUSE	34 kDa	0.77	0.08
Electron transfer flavoprotein-ubiquinone oxidoreductase	4-11	ETFD_MOUSE (+1)	68 kDa	0.72	0.09
Electron transferring flavoprotein, alpha	9-12	B1B1B4_MOUSE (+1)	35 kDa	0.86	0.09
Electron transfer flavoprotein subunit beta	8-12	ETFB_MOUSE	28 kDa	1.20	0.13
Enoyl-CoA hydratase	3-5	ECHM_MOUSE	31 kDa	1.31	0.13
Long-chain specific acyl-CoA dehydrogenase	10-12	ACADL_MOUSE	48 kDa	1.10	0.14
Carnitine O-palmitoyltransferase 1	3-8	CPT1B_MOUSE	88 kDa	0.71	0.15
Carnitine O-palmitoyltransferase 2	3-8	CPT2_MOUSE	74 kDa	0.76	0.18
Short-chain specific acyl-CoA dehydrogenase	3-5	ACADS_MOUSE	45 kDa	0.91	0.23
Trifunctional enzyme subunit alpha	22-27	ECHA_MOUSE	83 kDa	0.98	0.37
Total Fatty Acid Oxidation				**0.89**	**0.02**
Table S2 (cont.)	**#pep**	**Accession #**	**MW**	***Taz*^{KD}/WT**	***P***

Tricarboxylic Acid (TCA) cycle					
Malate dehydrogenase, mitochondrial	**16-18**	**MDHM_MOUSE**	**36 kDa**	**1.40**	**0.01**
Succinate-CoA ligase [ADP-forming] , beta	**7-10**	**SUCB1_MOUSE**	**50 kDa**	**0.82**	**0.02**
Protein Ogdhl - OGDH precursor	**2-9**	**E9Q7L0_MOUSE**	**117 kDa**	**0.62**	**0.02**
Aconitate hydratase, mitochondrial	27-31	ACON_MOUSE	85 kDa	1.30	0.08
Succinyl-CoA ligase subunit beta	2-4	E9Q2W0_MOUSE	45 kDa	1.39	0.14
Isocitrate dehydrogenase [NAD] subunit alpha	7-9	sp|Q9D6R2|IDH3A_MOUSE	40 kDa	1.15	0.19
DHL-residue succinyltransferase of OGDH	5-8	sp|Q9D2G2|ODO2_MOUSE	49 kDa	0.88	0.23
Citrate synthase	11-15	CISY_MOUSE	52 kDa	1.15	0.26
Isocitrate dehydrogenase 3 (NAD+) beta	2-3	Q91VA7_MOUSE	42 kDa	0.90	0.28
Isocitrate dehydrogenase [NADP], mito	20-24	IDHP_MOUSE	51 kDa	0.98	0.35
2-oxoglutarate dehydrogenase (OGDH)	19-22	sp|Q60597|ODO1_MOUSE	116 kDa	1.01	0.45
Fumarate hydratase	9-14	sp|P97807-2|FUMH_MOUSE	50 kDa	1.02	0.47
Succinyl-CoA ligase [ADP/GDP-forming] , alpha	3-6	SUCA_MOUSE	36 kDa	0.98	0.47
Isocitrate dehydrogenase [NAD] , gamma 1	4-7	IDHG1_MOUSE (+2)	43 kDa	1.01	0.49
Total TCA cycle				**1.16**	**0.01**
Malate-aspartate shuttle (mitochondrial proteins)					
Malate dehydrogenase	**16-18**	**MDHM_MOUSE**	**36 kDa**	**1.40**	**0.01**
Mitochondrial 2-oxoglutarate/malate carrier	**6-10**	**M2OM_MOUSE (+1)**	**34 kDa**	**0.80**	**0.03**
Aspartate aminotransferase, mitochondrial	10-15	AATM_MOUSE	47 kDa	1.14	0.18
Total Malate-aspartate shuttle				**1.30**	**0.02**
Pyruvate Dehydrogenase (PDH) complex					
Dihydrolipoyllysine acetyltransferase (E2)	**8-10**	**ODP2_MOUSE**	**68 kDa**	**1.43**	**0.00**
PDH E1 component subunit beta	7-9	ODPB_MOUSE	39 kDa	1.27	0.07
PDH E1 component subunit alpha	9-12	ODPA_MOUSE (+1)	43 kDa	1.08	0.31
Dihydrolipoyl dehydrogenase (E3)	8-10	DLDH_MOUSE	54 kDa	1.08	0.34
Total PDH complex				**1.20**	**0.01**
Amino acid and ketone oxidation					
Isovaleryl coenzyme A dehydrogenase	2-5	A3KGG9_MOUSE (+1)	46 kDa	0.83	0.27
Lipoamide acyltransferase of BCKDH	2-3	ODB2_MOUSE	53 kDa	1.12	0.34
3-hydroxyisobutyrate dehydrogenase	2-3	3HIDH_MOUSE	35 kDa	1.35	0.14
3-hydroxyisobutyryl-CoA hydrolase	3-6	HIBCH_MOUSE	43 kDa	1.37	0.17
D-beta-hydroxybutyrate dehydrogenase	3-6	BDH_MOUSE	38 kDa	1.14	0.32
Amino acid and ketone oxidation				1.18	0.09
ATP transport					
ADP/ATP translocase 1	15-20	ADT1_MOUSE	33 kDa	0.98	0.42
ADP/ATP translocase 2	2-5	ADT2_MOUSE (+1)	33 kDa	0.99	0.47
Creatine kinase S-type, mitochondrial	12-15	KCRS_MOUSE	47 kDa	0.89	0.08
ATP transport				1.07	0.30
Other significant differences					
Acyl-coenzyme A thioesterase 2	**5-12**	**ACOT2_MOUSE**	**50 kDa**	**1.88**	**0.00**
Acyl-coenzyme A thioesterase 13	**2-4**	**ACO13_MOUSE (+1)**	**15 kDa**	**1.90**	**0.01**
Stress-70 protein	**6-16**	**GRP75_MOUSE (+1)**	**74 kDa**	**2.04**	**0.02**
Lon protease	**2-11**	**E9Q120_MOUSE (+1)**	**106 kDa**	**3.53**	**0.00**

Proteins were quantified by LC/MS/MS as described in Methods with an FDR of 0.1%. Totals represent the spectral count sums of all proteins listed in the given complex or pathway. Spectral counts of bolded proteins and totals were higher (red) or lower (blue) in Taz^{KD} compared to WT at $P < 0.05$ by a Student's *t*-test with Benjamini-Hochberg correction for multiple comparisons ($q < 0.05$; FDR = 0.2). #pep = number of unique peptides assigned to each protein identified in each sample. Identification probability was 99.8-100% for all proteins listed (see raw data for percent sequence coverage for each protein at are available at https://doi.org/10.5281/zenodo.3932695.

SUPPLEMENTAL REFERENCES

1. Kall, L., Storey, J. D., MacCoss, M. J., and Noble, W. S. (2008) Assigning significance to peptides identified by tandem mass spectrometry using decoy databases. *J Proteome Res* **7**, 29-34
2. Keller, A., Nesvizhskii, A. I., Kolker, E., and Aebersold, R. (2002) Empirical statistical model to estimate the accuracy of peptide identifications made by MS/MS and database search. *Anal Chem* **74**, 5383-5392
3. Searle, B. C., Turner, M., and Nesvizhskii, A. I. (2008) Improving sensitivity by probabilistically combining results from multiple MS/MS search methodologies. *J Proteome Res* **7**, 245-253
4. Liu, H., Sadygov, R. G., and Yates, J. R., 3rd. (2004) A model for random sampling and estimation of relative protein abundance in shotgun proteomics. *Anal Chem* **76**, 4193-4201
5. Smith, C. A., Want, E. J., O'Maille, G., Abagyan, R., and Siuzdak, G. (2006) XCMS: processing mass spectrometry data for metabolite profiling using nonlinear peak alignment, matching, and identification. *Anal Chem* **78**, 779-787
6. Stein, S. E. (1999) An integrated method for spectrum extraction and compound identification from gas chromatography/mass spectrometry data. *Journal of the American Society for Mass Spectrometry* **10**, 770-781
7. Palladino, A. A., Chen, J., Kallish, S., Stanley, C. A., and Bennett, M. J. (2012) Measurement of tissue acyl-CoAs using flow-injection tandem mass spectrometry: acyl-CoA profiles in short-chain fatty acid oxidation defects. *Mol Genet Metab* **107**, 679-683
8. Dudek, J., Cheng, I. F., Chowdhury, A., Wozny, K., Balleininger, M., Reinhold, R., Grunau, S., Callegari, S., Toischer, K., Wanders, R. J., Hasenfuss, G., Brugger, B., Guan, K., and Rehling, P. (2016) Cardiac-specific succinate dehydrogenase deficiency in Barth syndrome. *EMBO Mol Med* **8**, 139-154